Effects of arm configuration on patterns of reaching variability in 3D space

by

Kishor Lakshmi Narayanan

A Thesis Presented in Partial Fulfillment
of the Requirements for the Degree
Master of Science

Approved July 2013 by the
Graduate Supervisory Committee:

Christopher Buneo, Chair
Marco Santello
Stephen Helms Tillery

ARIZONA STATE UNIVERSITY

August 2013

ABSTRACT

Reaching movements are subject to noise in both the planning and execution phases of movement production. Although the effects of these noise sources in estimating and/or controlling endpoint position have been examined in many studies, the independent effects of limb configuration on endpoint variability have been largely ignored. The present study investigated the effects of arm configuration on the interaction between planning noise and execution noise. Subjects performed reaching movements to three targets located in a frontal plane. At the starting position, subjects matched one of two desired arm configuration 'templates' namely "adducted" and "abducted". These arm configurations were obtained by rotations along the shoulder-hand axis, thereby maintaining endpoint position. Visual feedback of the hand was varied from trial to trial, thereby increasing uncertainty in movement planning and execution. It was hypothesized that 1) pattern of endpoint variability would be dependent on arm configuration and 2) that these differences would be most apparent in conditions without visual feedback. It was found that there were differences in endpoint variability between arm configurations in both visual conditions, but these differences were much larger when visual feedback was withheld. The overall results suggest that patterns of endpoint variability are highly dependent on arm configuration, particularly in the absence of visual feedback. This suggests that in the presence of vision, movement planning in 3D space is performed using coordinates that are largely arm configuration independent (i.e. extrinsic coordinates). In contrast, in the absence of vision, movement planning in 3D space reflects a substantial contribution of intrinsic coordinates.

TABLE OF CONTENTS

LIST OF TABLES

Table Page

LIST OF FIGURES

Chapter 1

INTRODUCTION

A voluntary movement is made when the motor system converts a desired goal into a plan of action and subsequently into muscle contractions required to complete that goal (Green and Kalaska, 2011). As illustrated in Figure 1A, neurons distributed in the supraspinal motor system convert the goal into motor commands as a feed-forward process and the spinal cord circuits transform these motor commands to muscle activity. The proprioceptive and visual system provides feedback to the motor system about the physical consequences of the motor command.

Sensorimotor processes convert a goal into a movement through a sequence of transformations from sensory inputs to the motor outputs (Figure 1B). It is believed that the motor systems implement these transformations via adaptive internal models (IMs) which are neural representations of the physical properties of the arm and its interactions with the world. The transformations start with the conversion of the target location input by the visual system into a desired reach trajectory. This trajectory is subsequently transformed to motor commands based on the properties of the IM which determine the computations required and also predict the physical consequences of those commands.

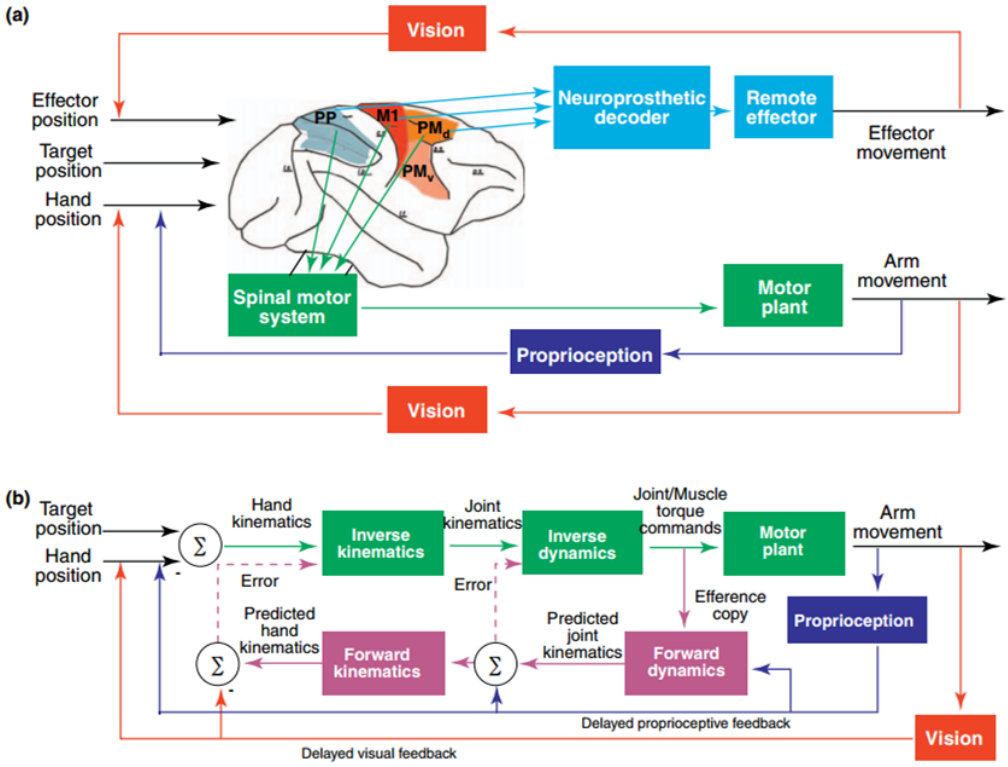

Figure 1. **Schematic of Control Systems and Block Diagram** (Green and Kalaska, 2011)

Variability in perception and action occurs from trial to trial even when external conditions such as the sensory input and goal are kept constant. This variability is attributed to noise at the neuronal level which affects every stage of sensorimotor processing (Faisal et al., 2008). Starting at sensory receptors, noise in sensory signals limits the amount of information delivered to the CNS. Noise is also found at the cellular level and in neurons in the form of electrical noise, especially channel noise from voltage-gated ion channels, which limits cell size and also produces trial to trial variability in action-potential initiation and propagation timing (Faisal et al., 2008). Finally, movement variability is also caused by noise in motor neurons due to their architecture which makes the conversion of motor commands to muscle contractions noisy (Faisal et al., 2008). These noises can be classified as noise that arise in part during

the transformation of sensory signals into motor commands ("planning noise") and in part during the transformation of motor commands into movements ("execution noise") (van Beers et al., 2004).

Planning noise arises in part from uncertainty during the initial sensing of the limb and target positions. Various studies have characterized how noise in visual and/or proprioceptive sensing contributes to this uncertainty (Osborne et al., 2005; Shi and Buneo, 2009; van den Dobbelsteen et al., 2001; Vindras et al., 1998). For example, noise arising during the sensing of limb positions is based on spatial characteristics of the individual sensors. Visual localization of the limb position was found to be precise when the limb was closer to the eye/body and in the azimuthal direction with respect to the cyclopean eye than localization in the radial direction (van Beers et al., 1998, 2002b). Proprioceptive localization of the hand in the radial direction with respect to the appropriate shoulder is more precise than localization in the azimuthal direction, and at hand positions at a shorter distance from the shoulder than more distant positions (van Beers et al., 1998, 2002b). Noise arising during other stages of planning such as during coordinate transformations or central integration of sensory signals also contributes to movement uncertainty (Gordon et al., 1994; McIntyre et al., 1997, 1998, 2000; Vindras and Viviani, 1998). This noise largely affects planning of movement direction and amplitude. Recent studies have also shown that variability in neuronal activity contributes to about one half of the variability in movement speed (Churchland et al., 2006).

Movement variability is also caused by execution-based noise. Buneo et al. (1995) found that the direction dependent movement variability caused by random fluctuations in magnitude of joint torques at the shoulder and elbow was different in

nature than variability caused by sensory noise. Recent studies also explored the effects of noise that were introduced directly into the motor commands (van Beers et al., 2004). They showed that when planning based noise is minimized, it effectively unmasks the effects of execution related noise in hand movement, the effect of which is highly movement direction dependent.

Though planning and execution based noise have typically been studied independently, they have been shown to interact naturally during movement (Thaler and Todd, 2009). A recent study by Faisal and Wolpert (2009) showed that planning and execution noise combine near optimally in the temporal domain. They demonstrated how sensory and motor variability depend on time and can be used to predict the overall task variability. That is, when sensing time is large, the variability in movement is largely indicative of the execution-based noise. This scheme can be extended to the spatial domain and can be argued that spatial distribution of endpoints during movement are not a result of planning noise alone but rather indicative of an interaction between planning and execution noise (Thaler and Todd, 2009). This was the case in studies where differences in the spatial distribution of planning and execution based noise determined differences in the endpoint variability in the presence and absence of hand vision (Apker et al., 2010; Apker and Buneo, 2012).

Although the effects of varying limb endpoint position have been examined in many studies, the independent effects of limb configuration have been largely ignored. Limb configuration is important in 3D arm movements as the mapping between endpoint position and arm posture is highly non-linear and affects both movement planning and execution (Soechting et al., 1995). In addition, different sets of muscles are responsible

for causing movement at different arm configurations. For example, the mechanical actions of muscles such as Anterior Deltoid, Middle Deltoid, Posterior Deltoid, Pectoralis major, and Latissimus dorsi change in a systematic way with changes in arm configuration (Buneo et al., 1996). As a result, the effects of planning and execution based noise likely differ substantially for different arm configurations.

In the present investigation, the effect of proprioceptively derived configuration cues on interaction between planning noise and execution noise was studied. Subjects were made to move from a single starting endpoint (fingertip) position to each of three targets located in a frontal plane. At the starting position, subjects were required to match one of two desired arm configuration 'templates'. These arm configurations, namely adducted and abducted, were obtained by rotations along the shoulder-hand axis, thereby maintaining endpoint position. Online visual feedback of the hand was also varied on a trial by trial basis, thereby increasing uncertainty in movement planning and execution. It was hypothesized that 1) patterns of endpoint variability would be dependent on arm configuration and 2) that these differences would be most apparent in conditions without visual feedback. These hypotheses were largely upheld: differences were found in endpoint variability between arm configurations in both visual conditions, but these differences were much larger when visual feedback of the hand was withheld. In other words, the absence of visual feedback and the increased uncertainty in arm configuration and position effectively revealed the effect of execution-based noise. The conclusion is that the endpoint variability is highly dependent on arm configuration in the absence of visual feedback.

Chapter 2

METHODS

Subjects

Ten subjects (8 men and 2 women) between the ages of 22 and 25 years were recruited to perform the experiment. Subjects were briefed on the experimental procedure, which involved reaching to targets in 3D space using the same starting position but different initial arm postures, but were naïve to the actual purpose of the experiment. The experiment was approved by the Arizona State University Institutional Review Board (IRB) before subject recruitment and data collection. Subjects read and signed an IRB approved informed consent form before participating in the experiment.

Apparatus

The experimental apparatus consisted of a large, standing metal frame that supported a 3D stereoscopic monitor (Dimension Technologies, Rochester, NY) as illustrated in Figure 2. The monitor projected images through an opening in the metal frame onto a mirror embedded in a metal shield. The metal shield was oriented at a 45° angle with respect to the monitor and enabled the subjects to see the projected images. The metal shield also served to block the arm from the subject's view. The subjects were made to position their heads on a chin rest to align their eyes to the center of the screen and were asked not to look away from the screen during the entire experiment.

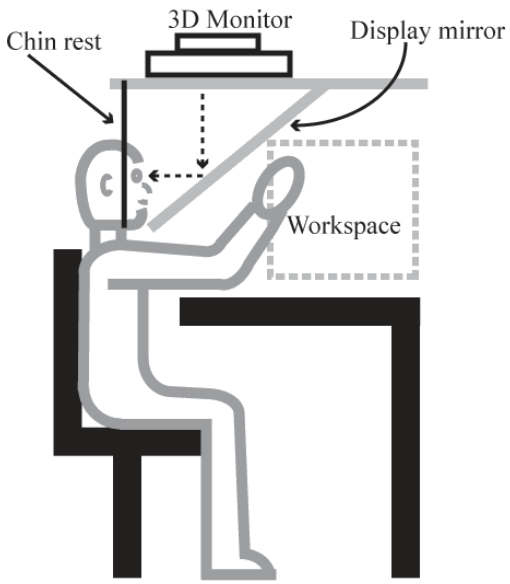

Figure 2. **Experimental Apparatus.** Schematic of the virtual reality set-up.

Motion Tracking

During the experiment, an active-LED-based motion tracking system was used to track movements of the arm (Visualeyez VZ-3000 motion tracker; Phoenix Technologies, Burnaby, British Columbia; 150-Hz sampling rate; 0.5-mm spatial resolution). LEDs were placed on the subject's fingertip, elbow and shoulder. The position of the fingertip LED was fed back to the subject in near real-time via a virtual reality environment developed in Vizard (WorldViz, Santa Barbara, CA). The fingertip position, starting position and targets were displayed as green spheres of ~5 cm diameter in the 3D monitor. To aid in depth perception, a wireframe cube was also rendered in the workspace. The starting position and the targets were contained within the cube.

The LEDs placed on the elbow, shoulder and the fingertip were used to compute and define the arm plane, the orientation of which concisely described the arm posture at the starting position (Soechting et al., 1995). The normal to the plane of the arm (**p**) was

first computed by finding the cross product of the vectors connecting the shoulder to elbow and elbow to fingertip:

$$\mathbf{p} = a \times b = (a2b3 - b3a2)i + (a3b1 - a1b3)j + (a1b2 - a2b1)k \qquad (1)$$

where $a = [a1\ a2\ a3]$ defines the vector connecting the shoulder to the elbow and $b = [b1\ b2\ b3]$ defines the vector connecting the elbow to the fingertip.

From this, the angle that **p** made with respect to the horizontal plane was calculated and monitored in real-time during the experiment.

Experimental Design

The subjects were given a task where they had to make reaching movements to one of three targets using one of two initial arm configurations and either with or without visual feedback of the fingertip. The targets were located in front of and above the starting position, requiring reaches upward and in depth from the starting position. The starting position was illuminated for 1.5 seconds at the start of each trial. The subject was given this time to align their fingertip to the starting position. Once they held their fingertip at the starting position for 350ms a target was illuminated cueing the movement. Vision of the fingertip was available to the subject throughout the movement on V trials and visual feedback of the fingertip position was removed at movement onset on NV trials. Feedback condition (V, NV) and target locations were pseudo randomly selected on trial by trial basis.

Trials were organized into blocks of 12 trials, with each block requiring the subject to reach to each of the three targets four times (two V trials and two NV trials). Each block of 12 trials involved a different initial arm configuration. Two different arm postures namely “adducted” and “abducted” were used in the experiment. An angle of 0°

indicated that the arm was adducted and 90° indicated abduction. However, an acceptable window of angles (0°-20° for adducted and 70°-90° for abducted) was given for the subjects to be considered that the subject was maintaining the required arm position. The subjects were instructed to hold the arm posture within the required window at the beginning of each trial as they aligned their fingertip with the starting position and to maintain that posture until the target was displayed. The arm postures were alternated for each block of trials with equal rest periods given between each block. This was to reduce fatigue due to elevating the limb for extended periods, which could affect performance of the subject.

Subjects had no knowledge of the trial parameters and were given instructions to move as quickly and accurately to the targets and to avoid making adjustments to fingertip position near the target at the end of the sequence. A trial was considered successful if the subject maintained the arm posture and reached a target quickly and stayed for 350ms within an acceptable window around the target. An auditory cue let the subjects know if a trial was successful. If the subject failed to reach a target, the trial was aborted and repeated later during the session.

Data Analysis

The movements were first sorted according to subject, feedback condition and arm posture. From this the movement data were smoothed using a digital low-pass filter.

Constant errors were calculated to assess movement accuracy by subtracting the known target location with the endpoint of the hand. However, since variable errors give more direct information about planning- and execution-related noise (McIntyre et al.,

1998; Carrozzo et al., 1999; van Beers et al., 2004) variable errors were calculated as follows:

$$\sigma_d = \frac{1}{n_d}\sqrt{\sum_{i=1}^{n_d}(h_d^i - \overline{h_d})^2} \qquad (2)$$

where $\overline{h_d}$ represents the mean endpoint position for a given target *d*. h_d^i represents the corresponding endpoint position on trial *i*, and n_d is the number of trials.

Ellipsoids were constructed around each endpoint distributions and Principal Components Analysis (PCA) was also used. Endpoint distributions associated with the frontal and depth sequences were compared by analyzing differences in the sizes, and shapes of their corresponding ellipsoids and orientation of each endpoint distributions derived from the PCA. The size of each ellipsoid was quantified by its volume (*V*):

$$V = \frac{4\pi}{3}xyz \qquad (3)$$

where *x* represents the radius of the major axis of the ellipsoid and *y* and *z* the minor axes. The shape of the ellipsoid was characterized by the ratio of the major axis to the sum of the radii of the minor axes. The general orientation of the endpoints was defined by the first eigenvector derived from the PCA (Carrozzo et al., 1999; McIntyre et al., 1997, 1998).

Statistical analyses

The angle of rotation between the first eigenvectors of the two vision conditions was computed separately for each arm posture. A nonparametric multi-sample test for equal medians in circular data (equivalent to the Wilcoxon signed-rank test for non-circular data) was used to test whether angle of rotation differed from zero. This would mean that there were differences in variability between vision conditions for each arm

posture. In addition, the angle of rotation between the first eigenvectors of the two arm configurations was computed separately for vision and non-vision conditions. The same test was used to show whether the rotation angle differed from each other for every posture in V and NV conditions.

Chapter 3

RESULTS

Figure 3 illustrates the movement paths and movement endpoints for the three different targets. Data from a single subject in the V condition for the two arm configurations are shown. The plots are shown from a 'top down' and 'frontal' view with ellipsoids constructed around each endpoint distribution. Figure 3A shows the paths and endpoint distributions for the adducted posture. The endpoint distributions are relatively consistent across targets as seen from the aspect ratio of the ellipsoids. The largest component of the distribution is seen to be aligned with the depth axis. Figure 3B shows the endpoint distributions for the abducted posture to be aligned with the depth axis as well. These trends were consistent across subjects in the V condition.

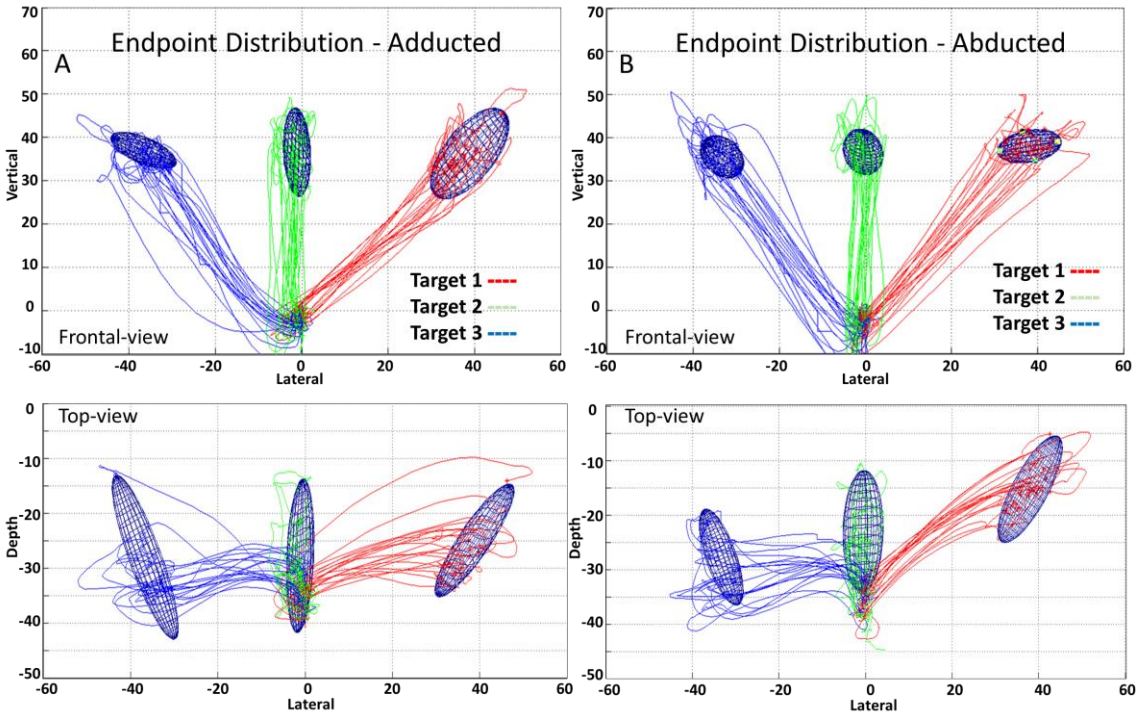

***Figure 3*. Endpoint distributions and hand movement paths in the V condition.** A: 'top view' and 'frontal view' of the hand movement paths and endpoint distributions in adducted posture. B: 'top view' and 'frontal view' of the hand movement paths and endpoint distributions in abducted posture.

The tendency for the movement variability to be distributed largely along the depth axis can also be appreciated from the orientation of the first eigenvectors derived from PCA. Figure 4 shows the primary (thick red bars) and secondary principle components (thick blue bars) for the same subject shown in Fig. 3. The orientation of the primary principle component is seen to be very consistent between the two arm positions for a given target. For all targets these vectors generally had their largest component along the depth axis.

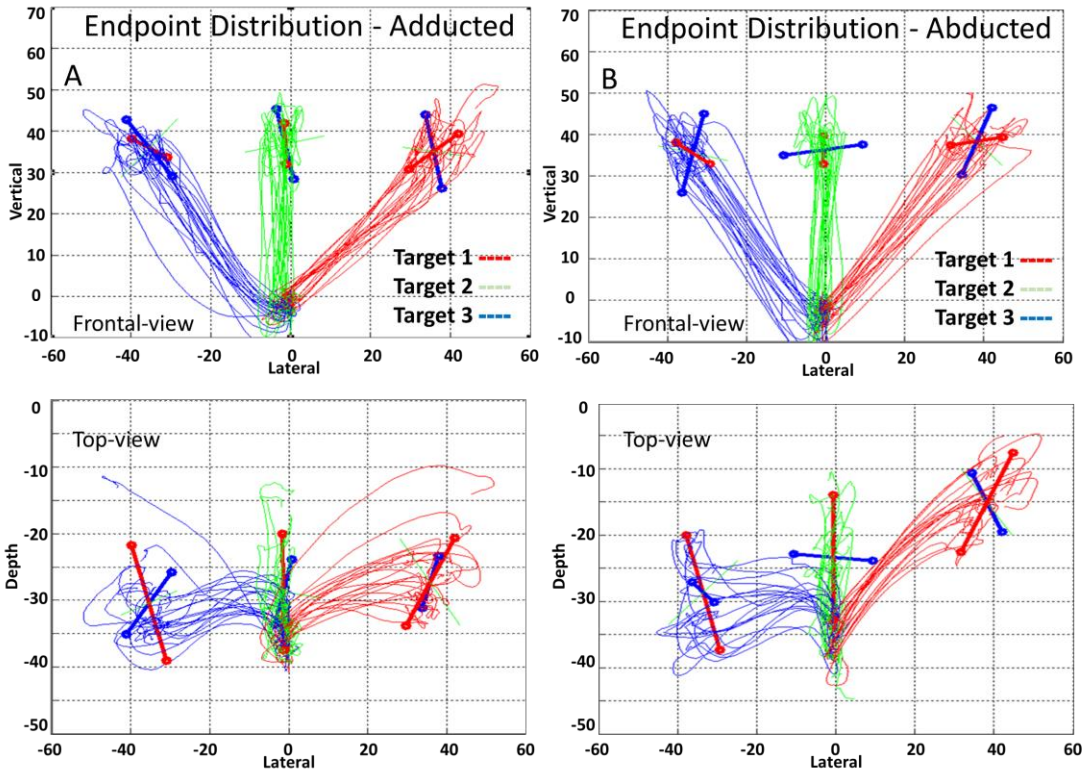

Figure 4. **Endpoint distributions and hand movement paths in the V condition with the primary principle component derived from PCA shown in red lines and the secondary principle component shown in blue lines.** A: 'top view' and 'frontal view 'of the hand movement paths and endpoint distributions in adducted posture. B: 'top view' and 'frontal view' of the hand movement paths and endpoint distributions in abducted posture. The first eigenvectors derived from PCA are shown as red lines. As with the ellipsoids the vectors are aligned along the depth axis

Figure 5 shows the components of the first eigenvectors associated with each endpoint distribution and arm posture for the same subject shown in Figs. 3 and 4. The

first eigenvectors are strongly biased along the depth axis and this is consistent in both adducted and abducted postures. Also, the relative magnitudes of the other eigenvector components were found to be similar between the arm postures. This can also be seen in the data from a different subject (Figure 6) and also at the population level.

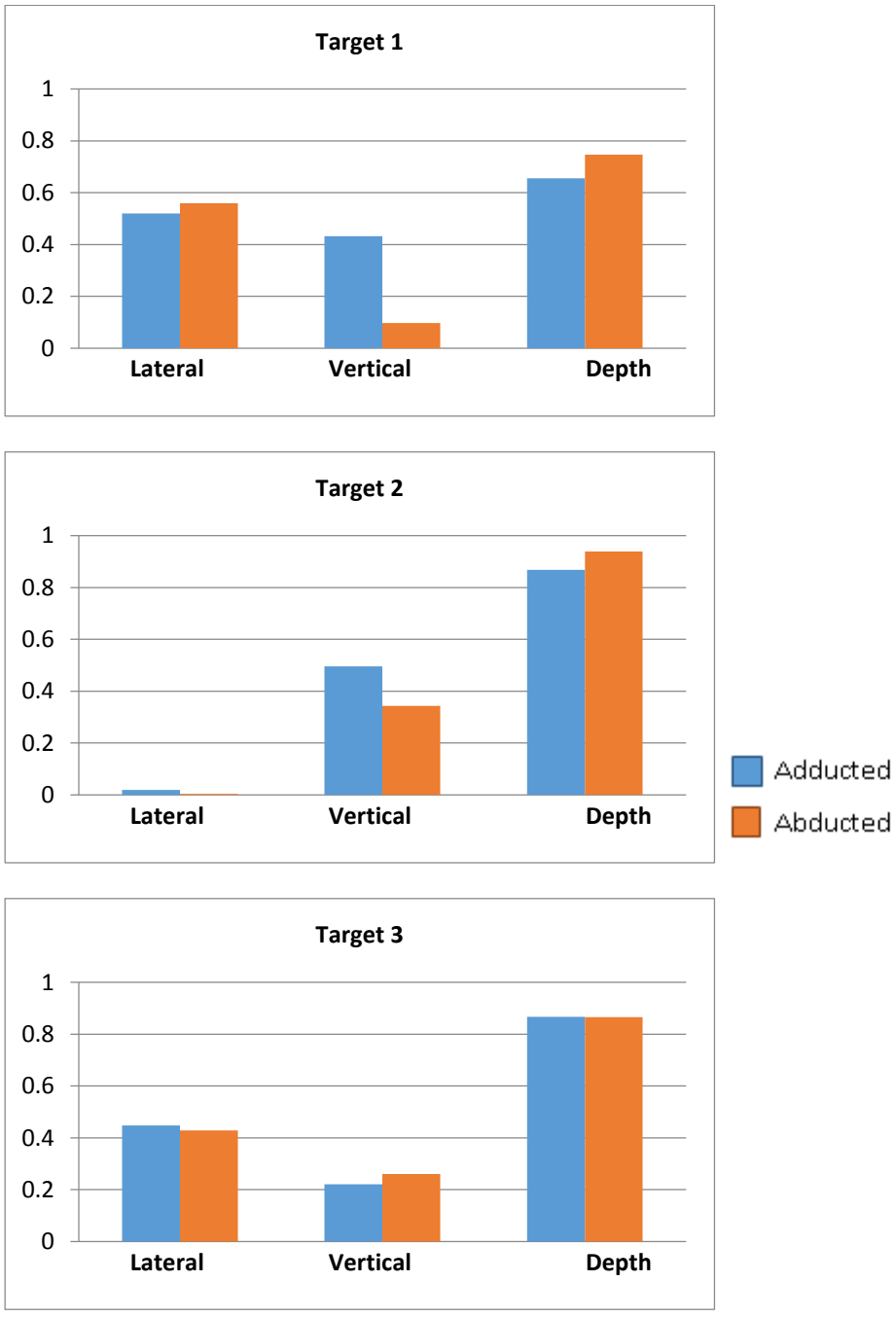

Figure 5. **Individual components of the first eigenvectors from Fig. 4.** The magnitudes are higher for the depth axis than the other axes. The magnitudes are quite similar across the two arm configurations.

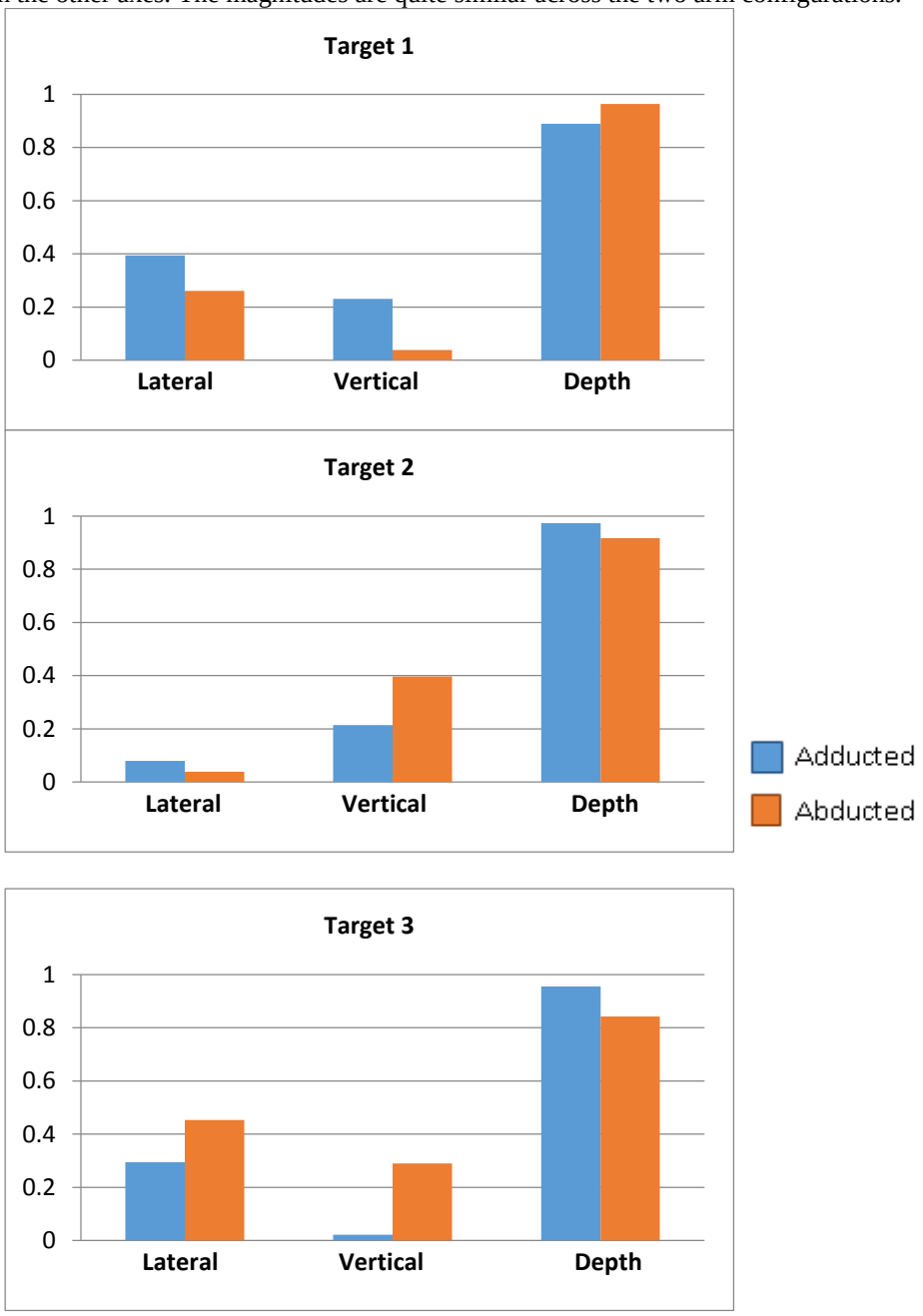

Figure 6. **Individual components of the first eigenvectors for a different subject.** As in Fig. 5 the magnitudes are higher for the depth axis than the other axes. The magnitudes are quite similar across the two arm configurations.

As in Fig. 3, Figure 7 shows the movement paths, endpoint distribution and ellipsoids for the same subject in NV condition. Comparatively, the endpoint

distributions for the non-visual condition are larger than in the V condition. This likely resulted from the increased uncertainty in estimating the hand position in the absence of visual feedback. The distribution shows that the largest component are not mostly aligned with the depth axis in both the adducted and abducted postures.

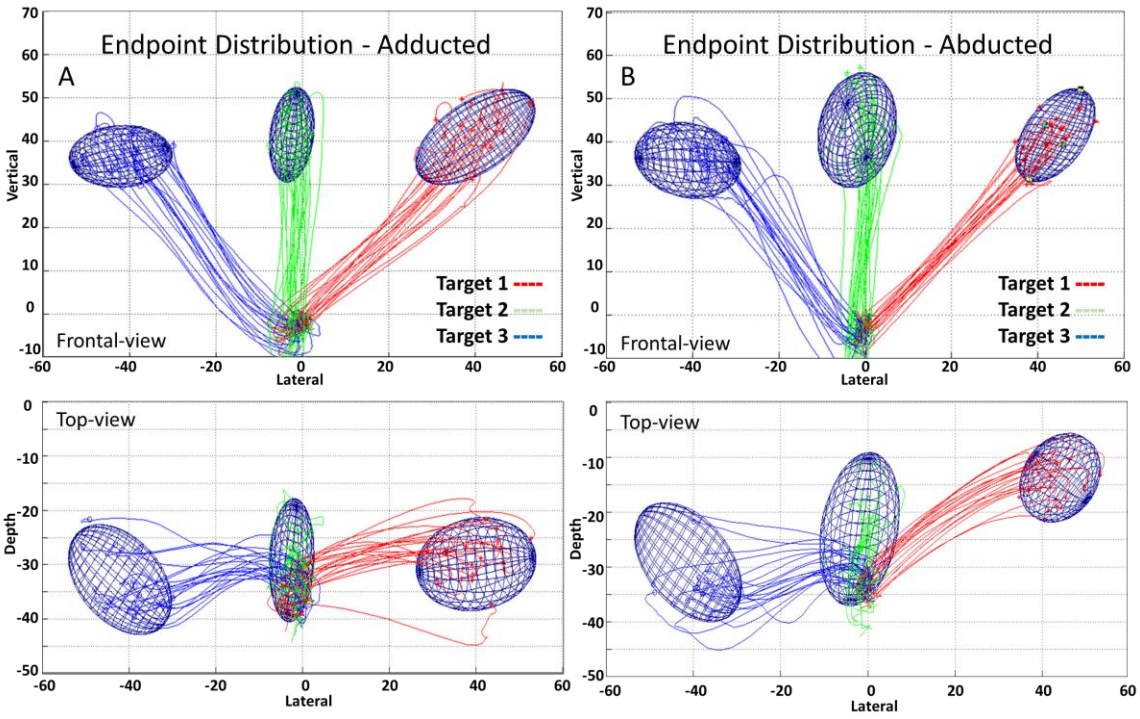

Figure 7. **Endpoint distributions and hand movement paths in the NV condition.** A: 'top view' and 'frontal view' of the hand movement paths and endpoint distributions in adducted posture. B: 'top view' and 'frontal view' of the hand movement paths and endpoint distributions in abducted posture. The ellipsoids are constructed around the endpoint distribution. The ellipsoids are larger signifying a larger distribution and are not mostly oriented along the depth axis.

The first eigenvectors derived from PCA do not show the orientation to be along the depth axis consistently across targets and arm configurations in the NV condition (Figure 8). Even the magnitude of the eigenvector components shown in Figure 9 are more similar to each other across axes in this condition than in the V condition. They do not seem particularly biased towards the depth axis. Also the magnitude of the individual

components vary largely between arm postures. This is consistently seen in the data from the other subject in Figure 10 and also at a population level.

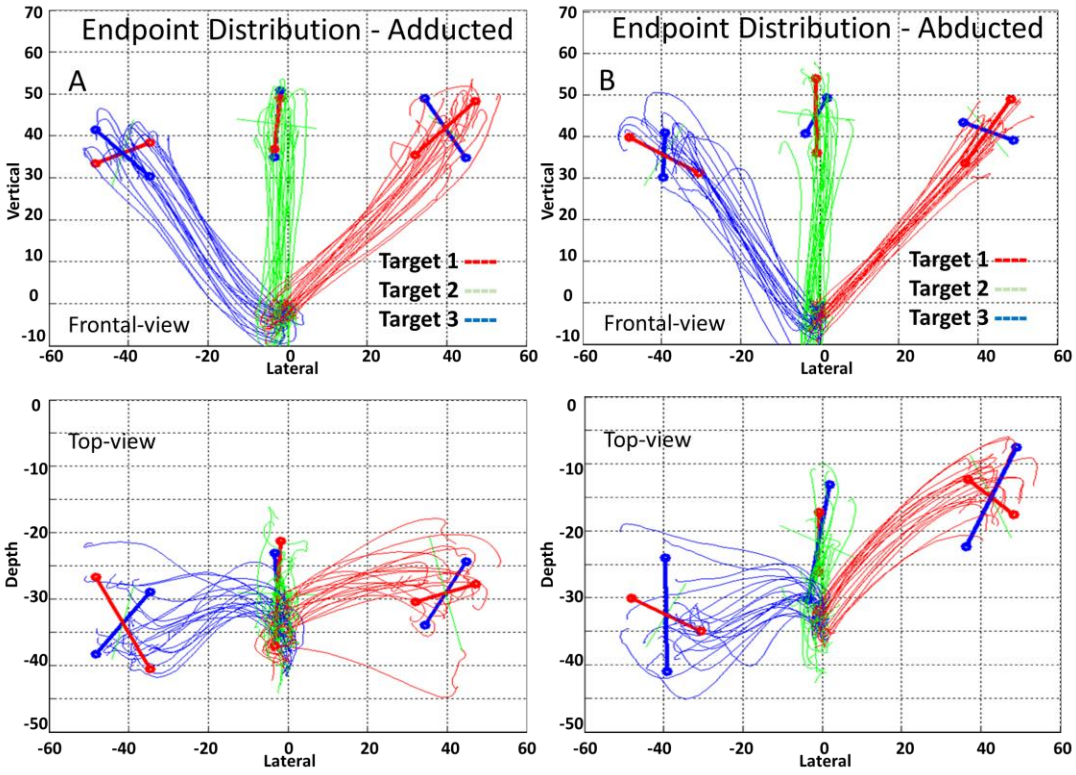

Figure 8. **Endpoint distributions and hand movement paths in the NV condition with the first eigenvectors derived from PCA shown as red lines**. A: 'top view' and 'frontal view' of the hand movement paths and endpoint distributions in adducted position. B: 'top view' and 'frontal view' of the hand movement paths and endpoint distributions in abducted posture. As with the ellipsoids the vectors are not aligned with the depth axis consistently.

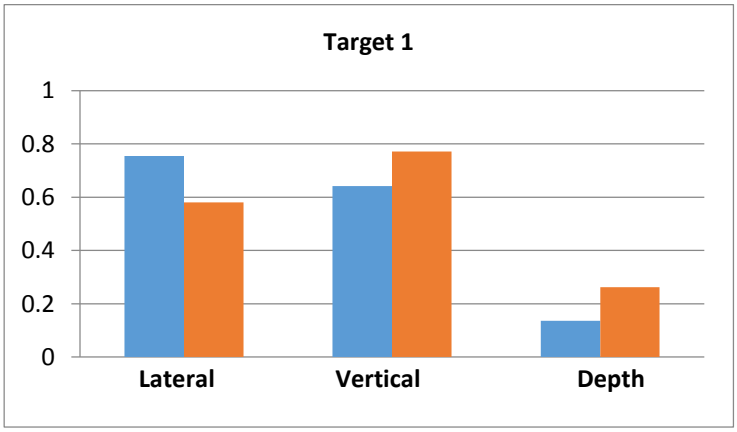

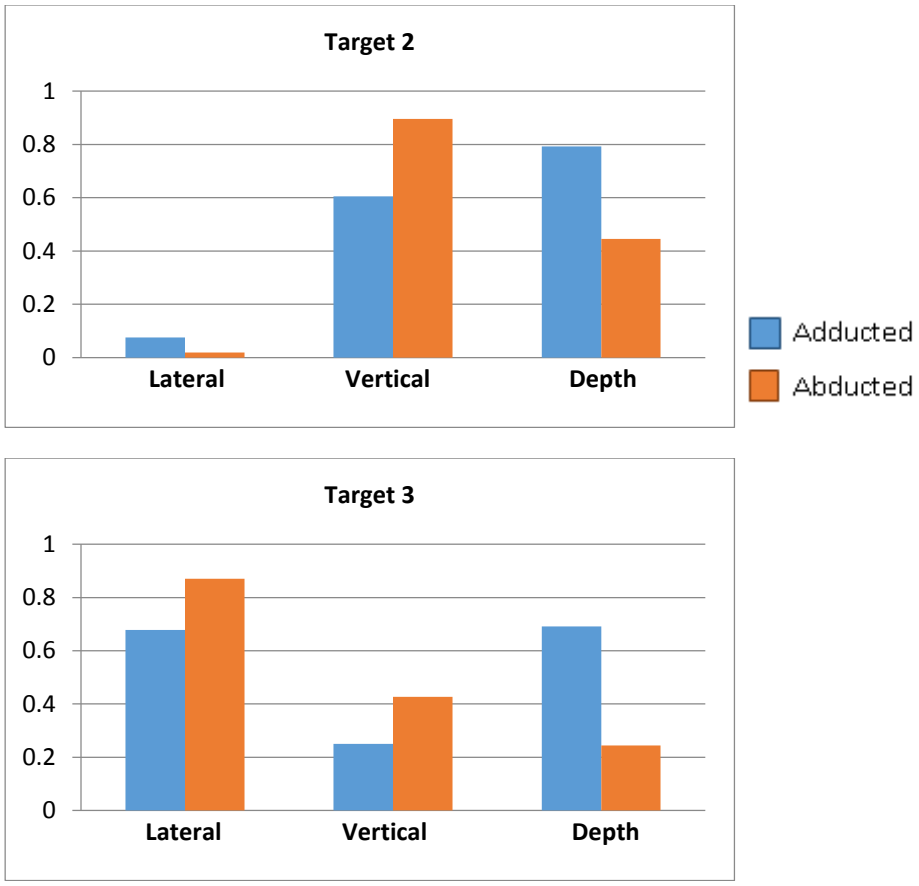

Figure 9. Individual components of the first eigenvectors from Fig. 8. The magnitudes are not biased towards the depth axis and vary considerably across arm postures.

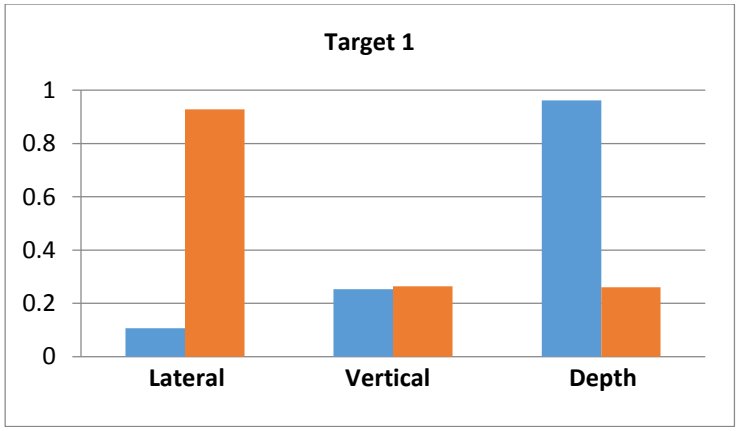

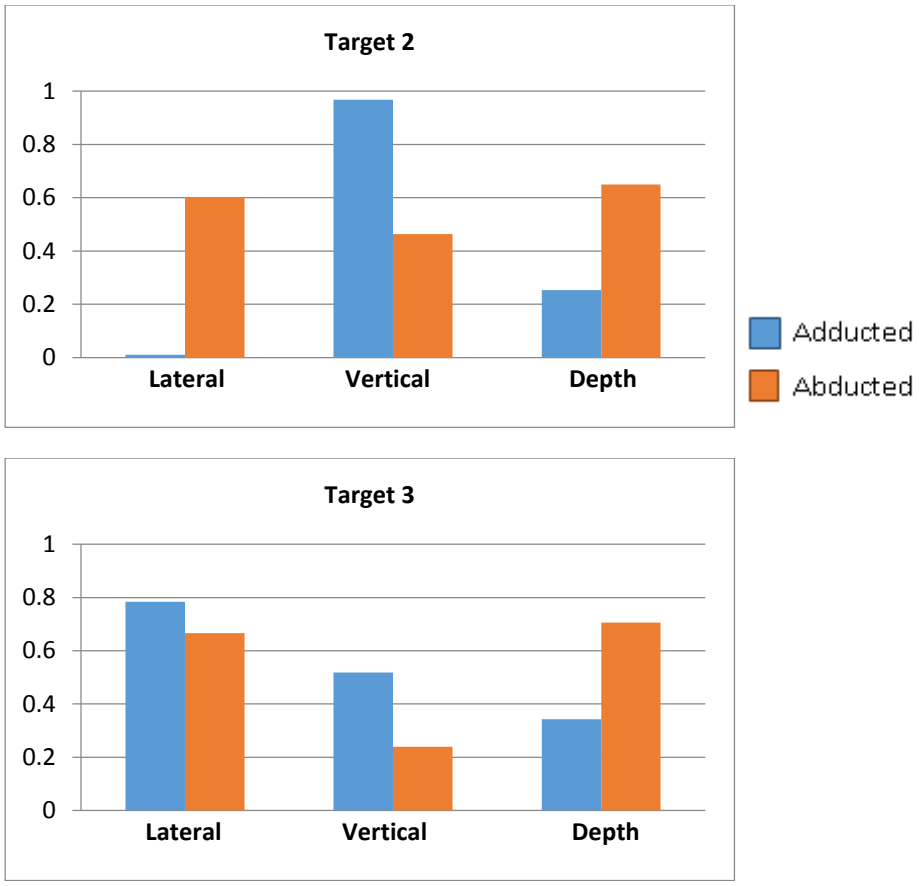

Figure 10. Individual components of the first eigenvectors for a different subject. The magnitudes are not biased towards the depth axis and vary considerably across arm postures as in Fig. 9.

In order to summarize the similarities and differences in variability between visual conditions, the angles of rotation between the first eigenvectors of the two visual conditions were computed for all three targets across all subjects. The rotation angles for each arm posture is illustrated in Figure 11. The boxplot shows that the rotation angle lies above zero for both arm postures which indicates that there were differences in variability between visual conditions for the two arm postures, consistent with Apker et al. (2010, 2012).

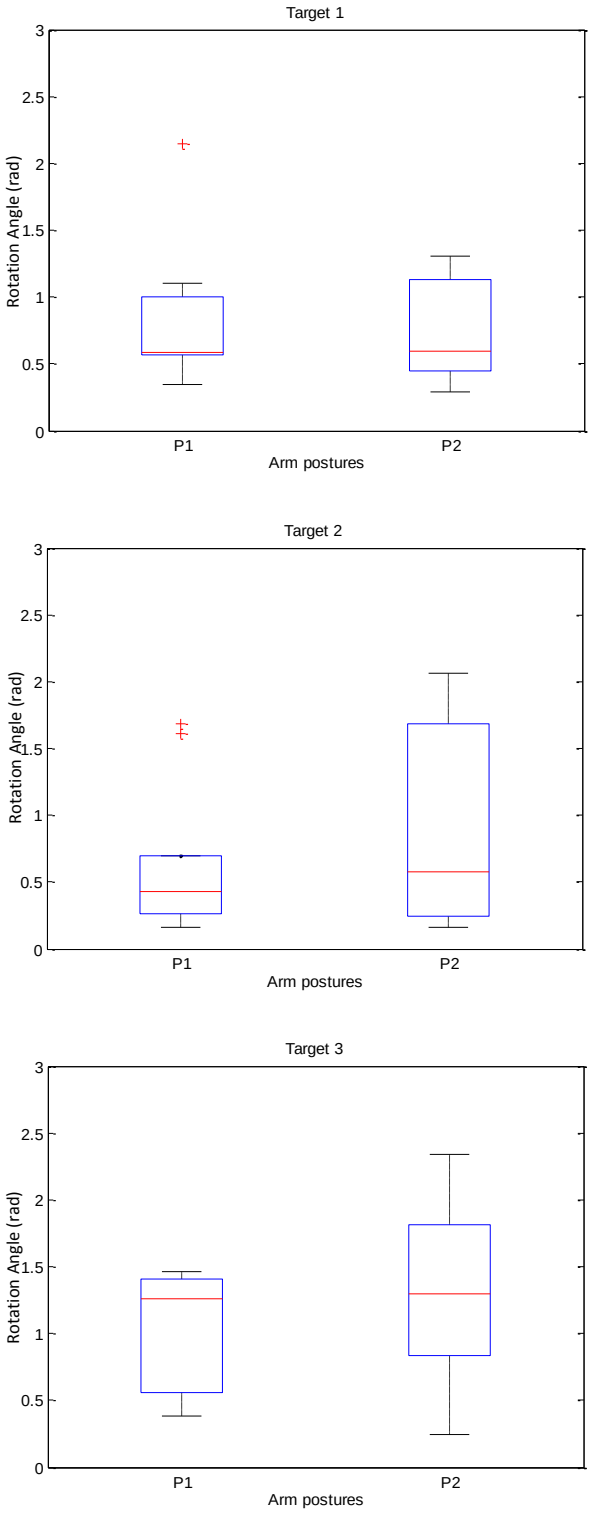

Figure 11. **Boxplots showing the rotation angles between the eigenvectors of the two visual conditions for each arm posture.** P1 is Adducted arm posture and P2 is Abducted arm posture.

In order to summarize the similarities and differences in variability between arm postures, the angles of rotation between the first eigenvectors of the two arm configurations were computed for all three targets across all subjects. The circular median of the rotation angles in each condition are illustrated in Table 1. This table shows them to be very low and similar across targets for the V condition. For the NV condition, the angles were also similar across targets but were generally much larger than in the V condition.

Table 1. Circular medians of the rotation angles between the first eigenvectors of the two arm postures for the visual conditions.

Circular medians of the rotation angles (rad)			
	Target 1	**Target 2**	**Target 3**
V condition	0.2118	0.1724	0.1675
NV condition	0.6629	1.0121	1.3326

Figure 12 illustrates the angles of rotation between arm postures for the two visual conditions. From the boxplot it is clearly evident that the rotation angle between the first eigenvectors of the two arm configurations is quite higher in the NV condition than in the V condition. This is also verified from the circular median values seen in Table 1. The circular medians are quite low and more similar across targets in the V condition than the NV condition. There is a clear difference between the medians in the NV and V conditions for each target. The difference is a bit smaller in target 1 than in target 2 and 3. Target 3 has the highest difference between the medians in NV and V conditions.

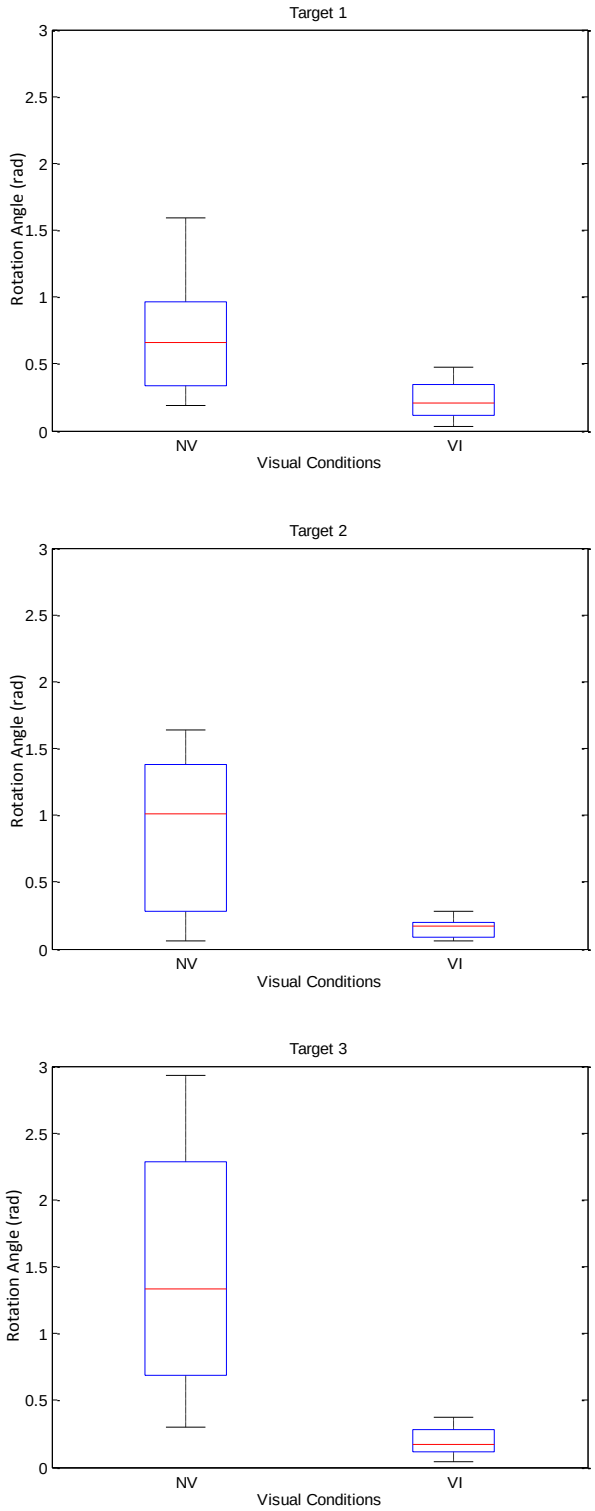

Figure 12. **Boxplots showing the angle of rotation between the first eigenvectors of the two arm postures for each visual condition.** NV is non-vision condition and VI is vision condition. The rotation angles are quite high between postures for non-vision conditions compared to the vision condition.

Chapter 4

DISCUSSION

In this experiment, the patterns of endpoint variability associated with movements performed with two different arm configurations at the start of these movements were quantified. For both arm configurations, movements were performed with and without vision of the hand. It was hypothesized that 1) patterns of endpoint variability would be dependent on arm configuration and 2) that these differences would be most apparent in conditions without visual feedback. It was found that in the presence of vision the endpoint distributions varied in orientation between arm postures. In the non-vision condition this was far more apparent, with the endpoint distributions highly varying for different arm postures. These results suggest that arm configuration influences endpoint variability. More specifically, in the absence of vision of the hand the increased uncertainty associated with estimating the position of the arm make the endpoint variability highly dependent on the arm configuration.

Relation to previous findings and significance. Previous studies have examined the roles of planning and execution related processes in determining movement variability for planar (2D) arm movements (van Beers et al., 2004; Gordon et al., 1994; Vindras et al., 1998). In addition, other studies have examined the factors contributing to movement variability in 3D space (Apker, 2010, 2012; Carrozzo et al., 1999; McIntyre, 1997, 1998; van den Dobbelsteen et al., 2001). Apker et al. (2010) examined the role of noise in determining variability in 3D arm movement sequences performed in the frontal plane and argued that patterns of movement variability were largely determined by visually derived noise associated with planning movements in depth. That is, endpoint

distributions were aligned to the depth axis and were very minimally influenced by the direction of hand movement and therefore execution noise. However, the fact that movements were orthogonal to the dominant axis of visual planning noise made it difficult to characterize the effects of execution noise in that study. As in Apker et al. (2010), Apker et al. (2012) examined the role of noise in 3D arm movements under conditions where visual feedback of the hand position was available and withheld from trial to trial. Here however, movements were either contained within a frontal plane or had large components in depth. The findings for the vision condition, and for the depth sequences in the NV condition, were largely consistent with the findings of both Apker et al. (2010) and McIntyre et al. (1997, 1998). However, the endpoint distributions for frontal sequences were strongly influenced by the primary axes of movement in the non-vision condition. This suggested that execution noise plays a more significant role in determining patterns of movement variability when visual feedback of the hand position is not available. The present investigation found results that were consistent with Apker et al. (2012). In the presence of vision, patterns of endpoint variability has their largest components along the depth axis. In the absence of vision, the increased uncertainty in estimating the arm position revealed the effects of execution noise in determining movement variability. That is, when vision of the hand was unavailable, patterns of endpoint movement variability were not generally aligned with the depth axis. This was true for both arm configurations.

None of the aforementioned 3D studies examined the effects of limb configuration in determining endpoint variability. A study by McIntyre et al. (1997) quantified the effects of different movement starting positions, effector hand, workspace

location, and head orientation in influencing movement endpoint distribution. The subjects made pointing movements to targets in 3D space after a memory delay for all these conditions. They found that the endpoint variability was anisotropic and independent of movement starting position. In the present investigation, the movement variability patterns were dependent on the starting arm posture in both the V and NV conditions, though this was particularly true in the NV condition. The overall results suggest that patterns of endpoint variability are dependent on arm configuration, particularly in the absence of visual feedback.

Previous work suggests that reaching movements directed to visually-defined targets are planned primarily within eye-centered coordinates and movements executed without vision appear to be planned in limb-based coordinates (Buneo & Andersen, 2006; Rushworth et al., 1997; Newport et al., 2001). The results from the present investigation provide strong evidence in support of this idea. That is, the results suggest that in the presence of vision, movement planning in 3D space is performed using coordinates that are largely arm configuration independent (i.e. extrinsic coordinates). In contrast, in the absence of vision, movement planning in 3D space reflects a substantial contribution of intrinsic coordinates.

Previous work has examined the effects of noise in estimating or executing changes in endpoint position ('extrinsic space') on variability. The present study was aimed at determining the extent to which movement variability reflects noise or uncertainty in intrinsic space. The results suggest the contribution of intrinsic factors is substantial but the results do not indicate whether this is due to noise/uncertainty in the estimation of arm posture (i.e. planning noise in intrinsic space) or due to noise in

sending motor commands to different sets of muscles associated with different arm postures (i.e. execution noise in intrinsic space). Future work will be aimed at addressing this important questions.

REFERENCES

Apker, G.A., Darling, T.K., & Buneo, C.A. (2010). Interacting noise sources shape patterns of arm movement variability in three-dimensional space. *Journal of neurophysiology, 104*, 2654 - 2666.

Apker, G.A., & Buneo, C.A. (2012). Contribution of execution noise to arm movement variability in three-dimensional space. *Journal of neurophysiology, 107*, 90 – 102.

Buneo C.A., & Andersen, R.A. (2006). The posterior parietal cortex: Sensorimotor interface for the planning and online control of visually guided movements. *Neuropsychologia, 44*, 2594-2606.

Buneo, C.A., Boline, J., Soechting, J.F., & Poppele, R.E. (1995). On the form of the internal model for reaching. *Exp Brain Res, 104*, 467 - 479.

Buneo, C.A., Soechting J.F., & Flanders M. (1997). Postural dependence of muscle actions: Implications for neural control. *Journal of Neuroscience, 17*, 2128 - 2142.

Carrozzo, M., McIntyre, J., Zago, M., & Lacquaniti, F. (1999). Viewer-centered and body-centered frames of reference in direct visuomotor transformations. *Exp Brain Res, 129*, 201 - 210.

Churchland, M.M., Afshar, A., & Shenoy, K.V. (2006a). A central source of movement variability. *Neuron, 52*, 1085 - 1096.

Churchland, M.M., Yu, B.M., Ryu, S.I., Santhanam, G., & Shenoy, K.V. (2006b). Neural variability in premotor cortex provides a signature of motor preparation. *Journal of neuroscience, 26*, 3697 - 3712.

Faisal, A.A., Selen, L.P.J., & Wolpert, D.M. (2008). Noise in the nervous system. *Nat Rev Neurosci, 9*, 292 - 303.

Faisal, A.A., & Wolpert, D.M. (2009). Near optimal combination of sensory and motor uncertainty in time during a naturalistic perception-action task. *Journal of neurophysiology, 101*, 1901 – 1912.

Gordon, J., Ghilardi, M.F., & Ghez, C. (1994). Accuracy of planar reaching movements. 1. Independence of direction and extent variability. *Exp Brain Res, 99*, 97 - 111.

Green, A. M., & Kalaska, J. F. (2011). Learning to move machines with the mind. *Trends in neurosciences, 34*, 61-75.

McIntyre, J., Stratta, F., Droulez, J., & Lacquaniti, F. (2000). Analysis of pointing errors reveals properties of data representations and coordinate transformations within the central nervous system. *Neural Comput, 12*, 2823 - 2855.

McIntyre, J., Stratta, F., & Lacquaniti, F. (1998). Short-term memory for reaching to visual targets: psychophysical evidence for body-centered reference frames. *Journal of neuroscience, 18*, 8423 - 8435.

McIntyre, J., Stratta, F., & Lacquaniti, F. (1997). Viewer-centered frame of reference for pointing to memorized targets in three-dimensional space. *Journal of neurophysiology, 78*, 1601 – 1618.

Newport, R., Hindle, J.V., & Jackson, S.R. (2001).Vision can improve the felt position of the unseen hand neurological evidence for links between vision and somatosensation in humans. *Curr. Biol, 11*, 975 – 980.

Osborne, L.C., Lisberger, S.G., & Bialek, W. (2005). A sensory source for motor variation. *Nature, 437*, 412 - 416.

Rushworth, M.F.S., Nixon, P.D., & Passingham, R.E. (1997). Parietal cortex and movement I. Movement selection and reaching. *Exp Brain Res, 117*, 292 – 310.

Shi, Y., & Buneo, C.A. (2009). Exploring the role of sensor noise in movement variability. *IEEE Engineering in Medicine and Biology Society*. 4970 – 4973.

Thaler, L., & Todd, J.T. (2009). The control parameters used by the CNS to guide the hand depend on the visuo-motor task: Evidence from visually guided pointing. *Neuroscience, 159*, 578 – 598.

van Beers, R.J., Haggard, P., & Wolpert, D.M. (2004). The role of execution noise in movement variability. *Journal of neurophysiology, 91*, 1050 - 1063.

van Beers, R.J., Sittig, A.C., & van der Gon, J.J.D. (1998). The precision of proprioceptive position sense. *Exp Brain Res, 122*, 367 - 377.

van Beers, R.J., Wolpert, D.M., & Haggard, P. (2002b). When feeling is more important than seeing in sensorimotor adaptation. *Curr Biol, 12*, 834 - 837.

van den Dobbelsteen, J.J., Brenner, E., Smeets, J.B.J. (2001). Endpoints of arm movements to visual targets. *Exp Brain Res, 138*, 279 - 287.

Vindras, P., Desmurget, M., Prablanc, C., & Viviani, P. (1998). Pointing errors reflect biases in the perception of the initial hand position. *Journal of neurophysiology, 79,* 3290 - 3294.

Vindras, P., & Viviani, P. (1998). Frames of reference and control parameters in visuomanual pointing. *J Exp Psychol Human, 24,* 569 - 591.